ARCHIVES of FOUNDRY ENGINEERING

Published quarterly as the organ of the Foundry Commission of the Polish Academy of Sciences

ISSN (1897-3310)
Volume 7
Issue 2/2007
119 – 124

25/2

The effect of copper concentration on the microstructure of Al-Si-Cu alloys

R. Maniara[a,*], L.A. Dobrzański[a], M. Krupiński[a], J.H. Sokołowski[b]
[a] Institute of Engineering Materials and Biomaterials, Konarskiego Str. 18A, 44-100 Gliwice, Poland
[b] Light Metals Casting Technology Group 401 Sunset Avenue, Windsor N9B 3P4, Ontario, Canada
*Corresponding author. E-mail address: rafal.maniara@polsl.pl

Received 08.02.2007; Approved for print on: 12.03.2007

Abstract

In the metal casting industry, an improvement of component quality depends mainly on better control over the production parameters. In order to gain a better understanding of how to control the as-cast microstructure, it is important to understand the evaluation of microstructure during solidification and understanding how influence the changes of chemical concentration on this microstructure. In this research, the effect of Cu content on the microstructure and solidification parameters of Al-Si-Cu alloys has been investigated. Thus, the thermal analysis of the alloys is used to control of aluminum casting process. The effect of different Cu content on solidification parameters such: aluminum dendrites nucleation temperature (T_{Liq}, Liquidus temperature), α+β eutectic nucleation temperature ($T_{E(Al+Si)N}$), Cu-rich eutectic nucleation temperature (T_{Al+Cu}), solidus temperature (T_{sol}), solidification range (ΔTs) has been studied in liquidus region. Influence of Cu content on the microstructure has been carried out. The principle observation made from this work ware that as copper concentration is increased the liquidus and solodius temperature decried. In addition to this it was observed that increase a Cu content from 1 to 4 wt % caused reduce of the secondary dendrite arm spacing and increase the grain size.

Keywords: Al-Si-Cu alloys; Effect of Cu concentration; Differential thermal analysis

1. Introduction

Al-Si-Cu alloy castings, made by variety of process and alloys, are widely used for automotive components. Alloy composition and casting process parameters are the most significant factors controlling the as-cast microstructure. The Al-Si-Cu alloy system is used in the production of engine components such as cylinder blocks and heads. At present the use of Al-Si-Cu alloy castings in this application is growing, replacing grey iron in many demanding applications [6].

A deeper understanding of the effect of the Cu content on the solidification process has to come to understand in recently years [1, 5, 9]. The effect of Cu content on the structural feature and thermal characteristic of Al-Si-Cu alloys has been investigated by many authors [1, 6, 8, 9, 12-14]. It is well known that Cu addition increases the strength of Al–Si–Cu alloys, which is due to the influence of Cu on the precipitation behavior of the alloys during the age-hardening treatment. So a further optimization of the mechanical properties of these foundry alloys can be expected by addition of Cu and optimized heat treatment.

The investigated Al-Si-Cu alloys are hypoeutectic Al-Si alloys with two main solidification stages, formation of aluminum reach (α-Al) dendrites fallowed by development of two phase eutectic (α-Al+Si). However, the additional alloying elements like as: Cu and Mg, as well as impurities like as: Fe, Mn, leads to

Table 1.
Reactions occurring during the solidification of the same AC AlSi6Cu3, (319.1) alloys according to Bäckerud [13] and Samuel [11]

Bäckerud et al. [13]	Temperature, ºC	Samuel et al. [11]	Temperature, ºC
(Al) dendrite network	609	(Al) dendrite network	610
L→(Al)+$Al_{15}Mn_3Si_2$+(Al_5FeSi)	590		
L→(Al)+Si+Al_5FeSi	575	Precipitation of eutectic Si	562
		Precipitation of $Al_6Mg_3FeSi_6$+Mg_2Si	554
L→(Al)+Al_2Cu+Al_5FeSi	525	Precipitation of Al_2Cu	510
L→(Al)+Al_2Cu+Si+$Al_5Mg_8Cu_2Si_6$	507	Precipitation of $Al_5Mg_8Cu_2Si_6$	490

Table 2.
Chemical composition of the alloys mentioned in this paper

	Average chemical composition, wt %					
	Si	Cu	Fe	Mn	Mg	Ti
Bäckerud et al. [13]	5,7	3,4	0,62	0,36	0,1	0,14
Samuel et al. [11]	6,23	3,8	0,46	0,14	0,06	0,14

more complex solidification reaction. Therefore, the Al-Si-Cu as-cast microstructure presents many intermetallic phases. Bäckerud [13] identified five reactions in alloy AC AlSi6Cu3 (319.1). The solidification reactions are listed in Table 1. For a similar alloy, Samule [11] proffered to indicate the new solid phases appearing at each characteristic temperature (Table 1). The compositions of the alloys are listed in Table 2.

The data presented in Table 1 show the two solidification sequence differ only slightly. After crystallization of Al-dendrites, Bäckerud identified the precipitation of phase $Al_{15}Mn_3Si_2$ probably together with Al_5FeSi, which wasn't detected by Samuel probably because of the smaller Mn content of the alloy used by the Samuel's. The eutectic Al+Si nucleation temperature for Samuel is significantly differs in these studies, 575 ºC for Bäckerud and 562 ºC for Samuel is agreement with the fact that this temperature is depressed by increasing the nominal Si content of the alloy. A slight thermal arrest at 554 ºC corresponding to the precipitation of $Al_6Mg_3FeSi_6$ and Mg_2Si could be detected by Samuel by comparison to their results on ACAlSi6Cu3 alloy with a high Mg concentration (0.5 wt.% [8] or according [13] 0,2 wt %) where this precipitations are easily observed.

Bäckerud recorded four phase Al+Al_2Cu+Si+Al_5FeSi reaction at 525 ºC. This reaction relates to the start of Al_2Cu precipitation [13]. According to Samuel this multi-phase compose should rather involve $Al_5Mg_8Cu_2Si_6$ together to Al_2Cu, somewhat in agreement with Backerud [13].The phase $Al_5Mg_8Cu_2Si_6$ appears in an invariant quaternary eutectic of Al-Cu-Mg-Si system which corresponds to the last reaction listed by Bäckerud (Table 1).

Many examinations have been cared out on the influence of Cu content on precipitation behavior of Al-Si-Cu and Al-Si-Cu-Mg alloys. It has founded that the addition of Cu influence on the increasing of the precipitation kinetics of β'' during artificial aging and refining the precipitate in the alloy [1]. The addition of Cu also changes the precipitation sequence of dispersoids in the alloys during artificial aging [1].

The Al_2Cu phase is observed such a bulk shape and in fine multi-phase eutectic-like deposits. These two shapes may be observed in castings cooled at very different cooling rates, with apparently a lower proportion of blocky precipitates as the cooling rate are increased [8, 11].

2. Materials and experimental procedure

2.1. Materials

Three (AC AlSi7Cu, AC AlSi7Cu2, ACAlSi7Cu4) experimental Al–Si–Cu alloys were produced at the University of Windsor (Canada) in the Light Metals Casting Laboratory, by melting the AC AlSi5Cu(Mg) base alloy and adding in proper proportion a AlCu55 and AlSi49 master alloys. The melted test samples were held for 12 hours in Lindberg™ electric resistance furnace at 850±5 ºC under a protective argon gas atmosphere. Before casting the melts were homogenized and degassed with the aim to reduce the hydrogen level below 0.100±0.005 ml H2/100g of aluminum and the surface was carefully skimmed. A total of 24 samples of the Al-Si-Cu alloys were prepared and thier chemical compositions were analyzed by Optical Emission Spectroscopy (OES) according to ASTM E1251 specification. The chemical compositions of these alloys are given in Table 3.

Table 3.
Average chemical composition of investigated alloys

Alloy label	Average chemical composition, wt %						
	Si	Fe	Cu	Mn	Mg	Zn	Ti
AC AlSi7Cu	7,166	0,1384	0,9901	0,11	0,268	0,0461	0,082
AC AlSi7Cu2	6,982	0,1687	1,91	0,0102	0,2552	0,425	0,0901
AC AlSi7Cu4	7,449	0,1655	3,595	0,2544	0,2829	0,0515	0,1265

2.2. Thermal analysis procedure

Thermal analysis (TA) tests were made using the UMSA Technology Platform [15]. The TA test samples were cast into a 0,25 mm thick stainless steel cap. The mould was isolated at the top and bottom to allow for Newtonian type heat transfer only. A schematic of the experimental set-up for thermal analysis is depicted in Figure 1. In order to obtain statistical confidence, the TA experiments were repeated eight times for each alloy.

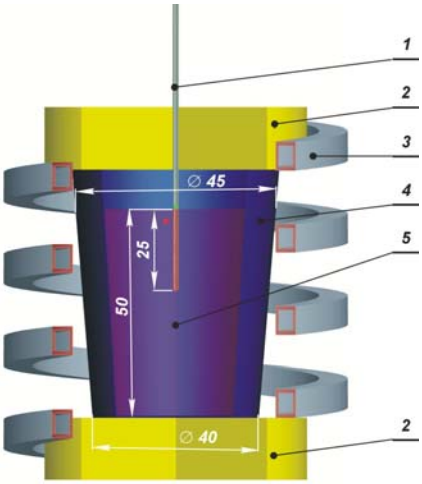

Fig. 1. Schematic of the UMSA Thermal Analysis Platform experimental set-up: 1 – low thermal mass thermocouple, 2 – thermal insulation, 3 – heating and cooling coil, 4 – steel mould, 5 – test sample

TA cooling curve was performed for all alloys using high sensitivity thermocouples of K type (Ni-Cr-Ni) that were protected in a stainless steel sheath and data were acquired by a high speed data acquisition system linked to a PC computer. The thermocouples were located in the centre of the crucible at a position of 25 mm from the top of the crucible. In order to obtain reproducible results, the thermocouple was placed exactly at the same position for each experiment. All experiments were performed at the room temperature (22 ºC) and barometric pressure (980 hPa). The cooling curve parameters considered in this work schematically shown in Figure 2. The aluminum dendrites network nucleation temperature – T_{DN}, the α+β eutectic nucleation temperature – $T_{E(Al+Si)N}$, Cu-rich eutectic nucleation temperature (T_{Al+Cu}), solidus temperature (T_{sol}), solidification range (ΔTs) were calculated using the first derivative of the cooling curve.

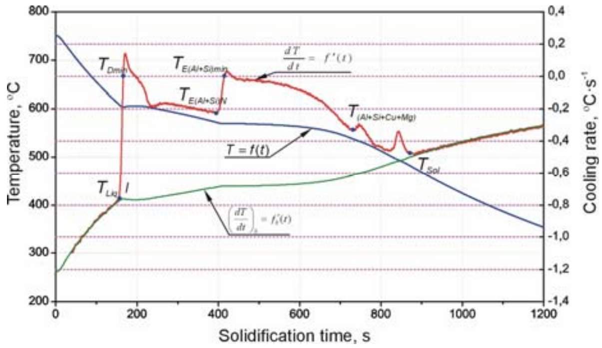

Fig. 2. Generic AC AlSi7Cu alloy cooling curve, firs derivative curve and representation of characteristic parameters used to analysis in the present examinations

2.3. Metallography and image analysis

The UMSA test analysis samples were cut longitudinally and then sectioned horizontally approximately 15 mm from the bottom and were prepared for metallographic analysis. Metallographic examinations have been made on investigated alloys specimens mounted in thermohardening resins. In order to disclose grain boundaries and the structure and to distinguish precisely the particular precipitations in Al–Si–Cu alloys as an etching reagent a 0,5–2 % of HBF_4 acid has been used. The observations of the investigated as-cast materials have been made on the light microscope LEICA MEF4A at magnification 500x, as well as on the electron scanning microscope Opton DSM-940 using a secondary electron detection. For comprehensive characterization of the Si structures a Leica Q-Win^{TM} and a Simagis Research^{TM} Image Analysis System were utilized.

The X-ray qualitative and quantitative microanalysis and the analysis of a surface distribution of cast elements in the examined Al–Si–Cu cast alloy specimens have been made on the Opton DSM-940 scanning microscope with the Oxford EDS LINK ISIS dispersive radiation spectrometer at the accelerating voltage of 15 kV and on the JEOL JCXA 733 x-ray microanalizer. Observations of thin foils structure were carried out in the JEM 3010UHR firmy JEOL transmission electron microscope using an accelerating voltage of 300 kV. Phase composition and crystallographic structure were determined by the X-ray diffraction method using the XPert device with a copper lamp, with 40 kV voltages. The measurement was performed by angle range of 2 Θ: 40-110º.

3. Results and discussion

3.1. Microstructure

As-cast microstructure of AC AlSi7Cu, AC AlSi7Cu2, AC AlSi7Cu4 alloys shows the typical solidification structure, having dendrites. Microstructure of the investigated alloys contains primary aluminum dendrites, eutectic silicon, iron-bearing intermetallics and copper-bearing intermetallics are shown on Figure 3. The analysis of thin foils have validated the fact that the structure of the investigating alloys consist of the solid solution α – Al (matrix) and an intermetallic secondary phase β – Si. The β – Si phase forms large flakes, needles and fibrous precipitations, depending on the Cu concentration. Moreover, the TEM examinations of the thin aluminum cast alloy foils confirm the existence of intermetallic phases: $AlFe_5Si$ and Al_2Cu (Figure 4) and didn't confirm the existence of intermetallic phases $Al_{15}Mn_3Si_2$ and Mg_2Si. The Al_2Cu phases solidify in two forms, block-like Al_2Cu (Figure 3 (brown particles) and Figure 4) and the finer eutectic-like $Al+Al_2Cu$ (Figure 3 c and Figure 5). The Al_2Cu block phases fraction is depending on the Cu content. Increasing the Cu content from 1 % do 4% increased the total of Al_2Cu block phases. The chemical composition examinations with the use of the EDS dispersive radiation spectrometer as well as literature data, confirm, that in investigated alloy occurring $Al_8FeMg_3Si_6$ phase (Figure 5 a, e).

Additional result of the surface distribution of elements and the x-ray, quantitative micro analysis made using the EDS energy dispersive radiation spectrometer show the presence of single Si crystals inside the $Al+Al_2Cu$ eutectic. This phase forms multicomponent eutectic with α–Al, β–Si and Al_2Cu (Figure 5).

According to the X–ray phase analysis, the ACAlSi7Cu and AC AlSi7Cu2 alloys are composed of two phases (Figure 6): α-Al solid solution as matrix and β-Si as a component of α+β eutectic or Si primary precipitation. The X-ray phase analysis don't ravel occurring of Al_2Cu, $AlFe_5Si$ and $Al_8FeMg_3Si_6$ phases, what suggested that the fraction volume of these phases is below 3% in these alloys. In addition the X-ray phases analyses made for an AC AlSi7Cu4 alloy confirmed the occurring of Al_2Cu phases. The distribution of the intermetallic phase is rather homogeneous.

a)
b)
c)

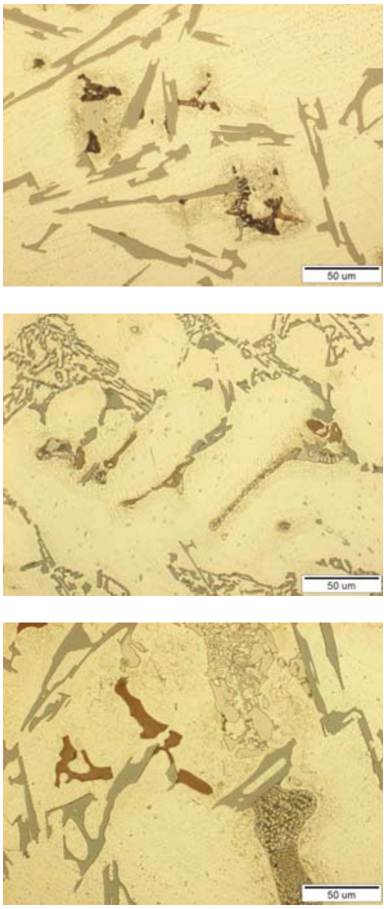

Fig. 3. Microstructure of the alloy containing: a) 1 % Cu, b) 2 % Cu, c) 4% Cu

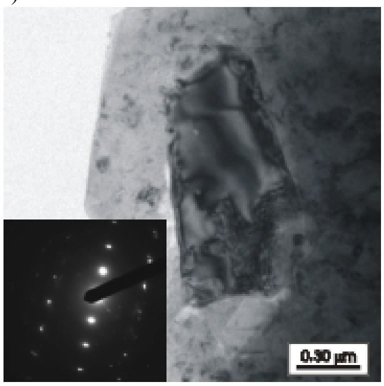

Fig. 4. TEM image of the AC AlSi7Cu4 alloy with selected area diffraction pattern

3.2. Thermo analyses

The first derivative curves recorded for the investigated alloys at various Cu contents are shown in Figure 7. Such is seen on the figure the shape of the first derivative curve is strongly depend on the Cu content. The number and shape of the peak visible in the Cu region is strongly relationship with the amount of Cu present in the alloy. As can be seen in Figure 7 an increasing in Cu content from 1 to 2 wt % postponed the Al+Si eutectic nucleation by more then 50 second. It can be observed that an increasing Cu content decreases the primary α-aluminum solidification time.

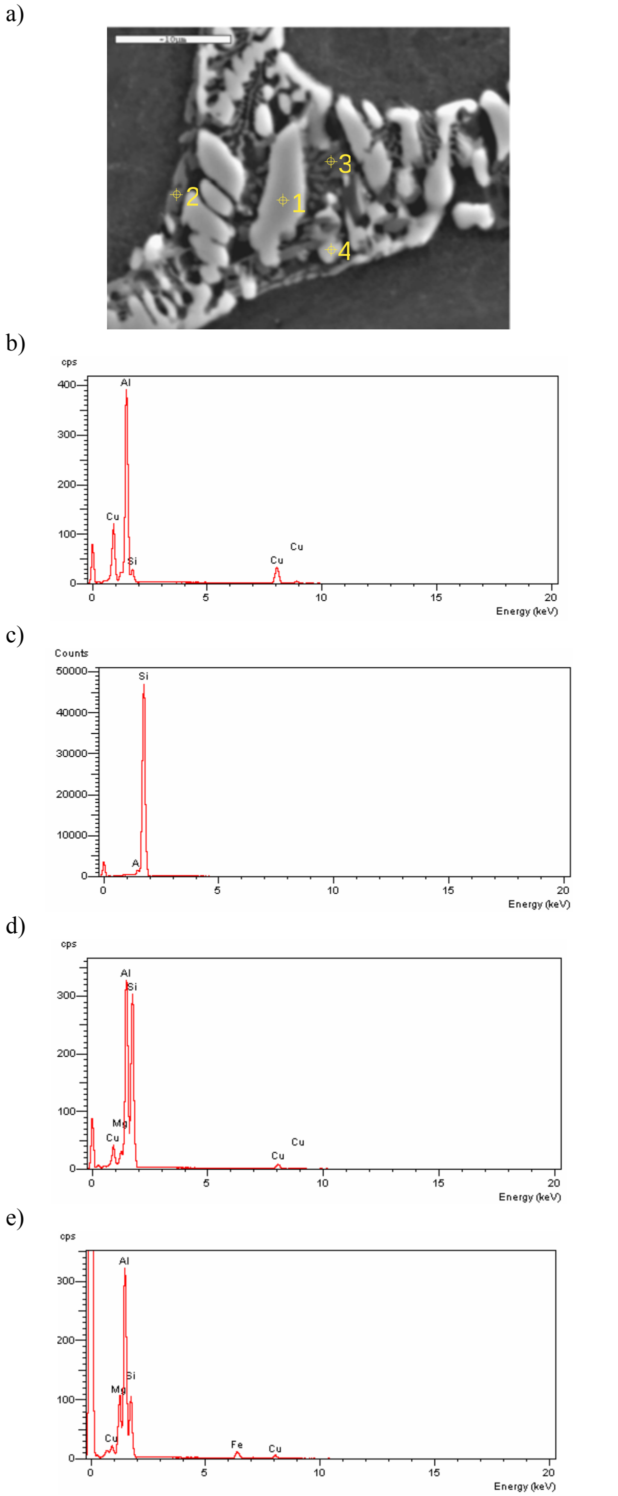

Fig. 5. a) SEM micrographs with characteristic morphology of Cu enriched phases, b) EDS analysis of phase no 1, c) EDS analysis of phases no 2, d) EDS analysis of phases no 3, e) EDS analysis of phases no 4 exhibited on figure a)

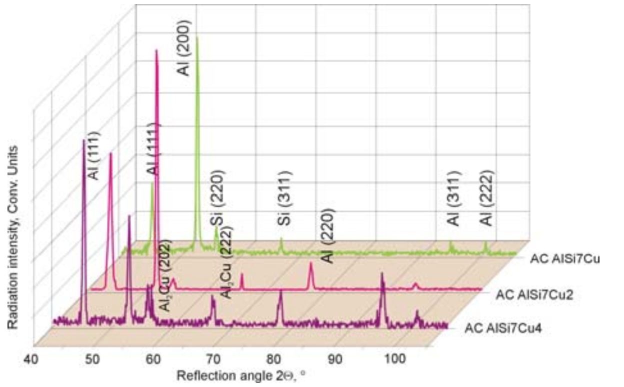

Fig. 6. XRD patterns of the AC AlSi7Cu, AC AlSi7Cu2, AC AlSi7Cu4 casting alloys

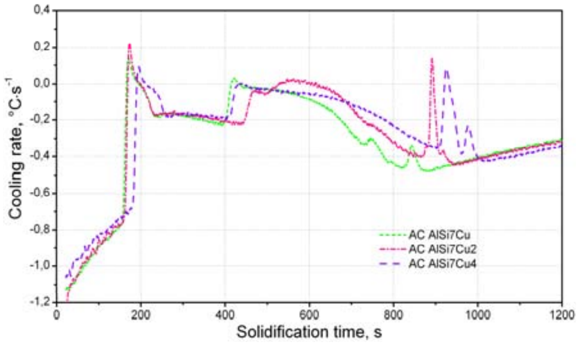

Fig. 7. First derivative crystallization curves at various Cu content

Increase the Cu content from 1 to 4% decreased the all phase transformation temperature (Figure 8). Although Cu content strongly affect on the precipitation of Cu enriched phases. When Cu content is increases from 1 to 4 wt % the precipitation temperature of the Cu enriched phases decreases (Figure 8). The Cu enriched phase represented by the first peak on the cooling curve (Figure 2 and 7) began to precipitate at 545 ºC for the AC Alsi7Cu alloy (Figure 8). For the AC AlSi7Cu2 alloy three peaks can be observed (Figure 7). One peak is dominated and the Cu phases represented by this peak began to precipitate at 529 ºC. Increasing the amount of Cu to 4 wt % (AC AlSi7Cu4 alloy) further changes the shape of the Cu enriched phase peaks. The precipitation temperature of these phases is also changed. The Cu enriched phase represented by this peak begins to precipitate at 499 ºC.

Increase the Cu content from 1 to 4 wt %increased total solidification time from 904 seconds for AC AlSi7Cu to 980 second for AC AlSi7Cu4.

4. Conclusion

Understanding of metal quality is of superior importance for control and prediction of casting characteristics. The results are summarized as follows:

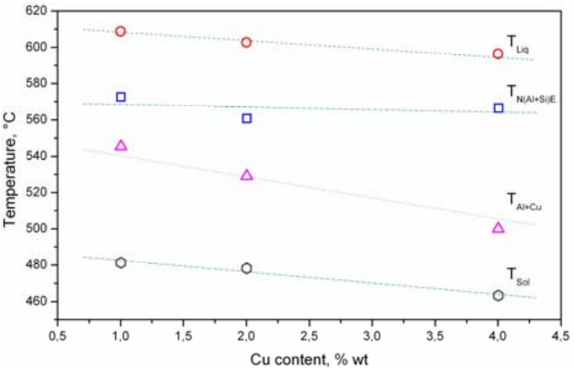

Fig. 8. of Cu content influence on the liquidus temperature (T_{Liq}), nucleation of Al+Si eutectic ($T_{N(Al+Si)E}$), nucleation of Al-Cu enriched phases (T_{Al+Si}) and solidus temperature (T_{Sol})

1. In investigated alloys there were identified five phases, which can suggest together witch thermal analysis, that in these alloys occur four solidification reactions listed below:

    a. (Al) dendrite network
    b. L→(Al)+Si+Al_5FeSi
    c. L→(Al)+Al_2Cu+Al_5FeSi
    d. L→(Al)+Al_2Cu+Si+$Al_5Mg_8Cu_2Si_6$

2. The phase transformation temperature depends on the Cu amount present in the investigated alloys. An increase of the Cu content from 1 to 4% decreases the investigated temperature values.

3. The nucleation temperature of Cu reach phases can be calculated from the first derivative curve for define maximum temperature of the conventional solution treatment.

Reference

[1] Y.J. Li, S. Brusethaug, A. Olsen, Influence of Cu on the mechanical properties and precipitation behavior of AlSi7Mg0.5 alloy during aging treatment, Scripta Materialia, Vol. 54 (2006), pp. 99-103.
[2] Ł. Bernat, J. Hajkowski, M. Hajkowski: Microstructure and porosity of aluminum alloy casting whereas mechanical properties, Archives of Foundry, Vol. 6, Issues 22 (2006), pp. 41-48 (in Polish).
[3] S. Pietrowski, R. Władysiak: Low-pressure casting process analysis of Al-Si car wheels casts, Archives of Foundry, Vol. 6, Issues 22 (2006), pp. 376-391 (in Polish).
[4] S. Pietrowski: Low- siliceous Al-Si alloys with Ni, Cu, and Mg additions, Archives of Foundry, Vol. 6, Issues 22, (2006), pp. 414-429 (in Polish).
[5] L. Y. Pio, S. Sulaimin, A.M. Hamouda: Grain refinement of LM6Al–Si alloy sand castings to enhance mechanical properties, Journal of Materials Processing Technology Vols. 162-163 (2005), pp. 435-441.
[6] J.G. Kauffman, E. L. Rooy: Aluminum Alloy Castings, ASM International, Ohio 2005.
[7] S.G. Shabestari, M. Malekan: Thermal Analysis Study of the Effect of the Cooling Rate on the Microstructure and Solidification Parameters Of 319 Aluminum Alloy, Canadian Metallurgical Quarterly, Vol. 44 (2005), pp. 305-312.
[8] E.J. Martı´nez, M.A. Cisneros, S. Valtierra, J. Lacaze, Effect of strontium and cooling rate upon eutectic temperaturesof A319 aluminum alloy, Scripta Materialia Vol. 52 (2005), pp. 439–443.
[1] Z. Li, A.M. Samuel, F.H. Samuel, C. Ravindran, S. Valtierra, H.W. Doty: Parameters controlling the performance of AA319-type alloys Part I. Tensile properties, Materials Science and Engineering, Vol. 367 (2004), pp. 96-110.
[9] S.G. Shabestari, H. Moemeni: Effect of copper and solidification conditions on the microstructure and mechanical properties of Al–Si–Mg alloys, Journal of Materials Processing Technology, Vols. 153-154 (2004), pp. 193-198.
[10] C.H. Cacers, M.B. Djurdjevic, T.J. Stockwell, J.H. Sokolowski, The effect of Cu content on the level of microporosity in Al–Si–Cu–Mg casting alloys, Scripta Materialia, Vol. 40 (1999), pp. 631–637.
[11] A. M. Samuel, A. Gotmare, F. H. Samuel: Effect of Solidification Rate and Metal Feedability on Porosity and SiC/Al_2O_3 Particle Distributing in an Al-Si-Mg (359) Alloy, Composite Science and Technology, 1994.
[12] L. Bäckerud, E. Król, J. Tamminen: Solidification Characteristics of Aluminum Alloys, Vol. 1, Universitetsforlaget, Oslo, 1986.
[13] L. Bäckerud, G. Chai, J. Tamminen: Solidification Characteristics of Aluminum Alloys, Vol. 2, American Foundry Society, Inc., Des Plaines, Illinois, 1992.
[14] L. Bäckerud, G. Chai: Solidification Characteristics of Aluminum Alloys, Vol. 3, American Foundry Society, Inc., Des Plaines, Illinois, 1992.
[15] http://www.uwindsor.ca/umsa.